GMR
The Original

FABRICATION OF MULTISCALE STARCH/PVA/CuO ELECTROSPUN NANOSCAFFOLDS FROM *Sargassum ilicifolium* (BROWN MARINE MACROALGAE) EXTRACT: PHYSICOCHEMICAL CHARACTERIZATION AND WOUND HEALING ASSESSMENT ON HaCaT CELLS

Manimegalai V[1], Karpaga Sundari C[2], Gohila B[3], Naijil George[4], Kamaraj Raju[5]*

[1]Department of Botany, A.V.V.M. Sri Pushpam College (Autonomous), Affiliated to Bharathidasan university, Poondi-613 503, Tamil Nadu, India. Email: vmanimegalai2017@gmail.com
[2]Department of Botany, A.V.V.M. Sri Pushpam College (Autonomous), Affiliated to Bharathidasan university, Poondi-613 503, Tamil Nadu, India. Email: sundarikarpagam1981@gmail.com
[3]Department of Zoology and Biotechnology, A.V.V.M. Sri Pushpam College (Autonomous), Affiliated to Bharathidasan university, Poondi-613 503, Tamil Nadu, India. Email: rowlinggohila@gmail.com
[4]Department of Biotechnology, St. Joseph's College (Autonomous), Irinjalakuda (Affiliated to the University of Calicut), Thrissur, Kerala-680121, India. Email: naijilgeorge@gmail.com
[5]School of Applied Biosciences, Food & Agri-Tech, Rathinam Global Deemed to be University, Coimbatore, 641021, Tamil Nadu, India. Email: kamaraj.lordshiva@gmail.com
*Corresponding Author: kamaraj.lordshiva@gmail.com (K.R.)

ABSTRACT
This study presents the development of novel bioengineered nanoscaffolds featuring copper oxide nanoparticles (CuO NPs) synthesized from algal extracts, specifically *Sargassum ilicifolium*, for advanced wound healing applications. Marine macroalgae were meticulously processed to yield bioactive-rich extracts, which facilitated the eco-friendly synthesis of CuO NPs with enhanced stability and biocompatibility. The resulting nanoparticles were embedded into starch/polyvinyl alcohol (PVA) electrospun nanofibrous mats, creating composite scaffolds with optimized physicochemical and mechanical properties. Comprehensive characterization—including UV-Vis spectroscopy, FTIR, XRD, SEM, TGA, and zeta potential analysis—confirmed successful nanoparticle integration and scaffold architecture. In vitro wound healing assays utilizing HaCaT keratinocytes demonstrated significantly improved cell migration and wound closure rates for the CuO-loaded scaffolds compared to control treatments, highlighting their potential as bioactive medical dressings. The synergistic combination of marine algal phytochemicals and biogenic CuO NPs in polymeric scaffolds offers a promising, sustainable strategy for accelerating tissue repair and regeneration. This research paves the way for clinically relevant, eco-intelligent wound care solutions based on marine biomaterials and green nanotechnology.

KEYWORDS: *Sargassum ilicifolium*, Green synthesis, CuO NPs, Starch/PVA/CuO-NPs nanoscaffolds, Wound-healing activity.

1. INTRODUCTION
Wound healing remains a critical challenge in healthcare due to the complex and dynamic biological processes involved in tissue repair [1]. Chronic wounds, often resulting from diabetes, infections, or prolonged inflammation, impose a significant burden on patients and healthcare systems worldwide [2]. Conventional wound dressings primarily offer passive protection and moisture retention, but recent advances emphasize the need for multifunctional wound care materials that not only act as physical barriers but also actively promote healing through antimicrobial activity, biocompatibility, and enhanced cellular regeneration [3]. In this context, nanotechnology-based biomaterials, particularly electrospun nanofibrous scaffolds, have emerged as promising candidates due to their structural similarity to the extracellular matrix (ECM), high surface area, and capacity to incorporate bioactive agents [4].
Among various polymers employed in scaffold fabrication, starch and polyvinyl alcohol (PVA) have garnered considerable attention due to their biocompatibility, biodegradability, and hydrophilicity [5]. Starch, a natural polysaccharide derived from plants, is inexpensive, renewable, and provides a favorable microenvironment for cell adhesion and proliferation [6]. PVA complements starch by improving mechanical strength, flexibility, and electrospinnability, enabling the fabrication of continuous nanofibers with tunable morphology [7]. The combination of starch and PVA in electrospun scaffolds thus offers an attractive platform for wound dressing applications [8]. However, to enhance the therapeutic potential of these scaffolds, the incorporation of bioactive nanoparticles capable of antimicrobial and antioxidant effects is essential [9].
Copper oxide nanoparticles (CuO NPs) have recently gained attention in biomedical research due to their potent antimicrobial properties against a wide spectrum of pathogens, including bacteria, fungi, and viruses [10]. Additionally, CuO NPs exhibit pro-angiogenic and anti-inflammatory effects that can accelerate wound healing

by promoting re-epithelialization and reducing oxidative stress [11]. The traditional chemical synthesis methods of CuO NPs often involve toxic reagents and harsh conditions that limit their biocompatibility and environmental sustainability [10]. Consequently, green synthesis approaches employing biological resources such as plant extracts, fungi, and algae have been increasingly adopted [12]. These eco-friendly methods utilize the natural reducing and stabilizing agents found in biological extracts to fabricate nanoparticles under mild conditions, producing biocompatible and functionally enhanced nanomaterials [13].

Marine macroalgae, particularly brown seaweeds like *Sargassum ilicifolium*, are rich sources of bioactive compounds including polyphenols, flavonoids, polysaccharides, and proteins [14]. These compounds possess antioxidant, anti-inflammatory, and antimicrobial activities, making *S.* species valuable for biomedical applications [15]. Moreover, the phytochemicals in *S.* extracts act as effective reducing and capping agents in the green synthesis of metallic nanoparticles, facilitating controlled particle size and morphology [16]. The use of ultrasonic-assisted extraction further improves the yield and efficacy of bioactive compounds by disrupting cell walls and enhancing solvent penetration, thereby optimizing the nanoparticle synthesis process [17].

The integration of biogenically synthesized CuO NPs into starch/PVA electrospun nanofibers creates a multifunctional wound dressing that can simultaneously provide structural support, sustained release of therapeutic agents, and protection against microbial invasion [18]. Electrospinning technology allows for the fabrication of nanoscaffolds with high porosity and interconnected pores, mimicking the native ECM and supporting cell migration and proliferation [19]. Such composite scaffolds can modulate the wound microenvironment, accelerating healing through synergistic effects of the polymer matrix and embedded nanoparticles [20].

Despite the promising attributes of marine algae-mediated green synthesis of nanoparticles and starch/PVA nanofibers individually, few studies have explored their combined potential in wound healing applications [21]. This study focuses on the development and characterization of multifunctional nanofibrous mats composed of starch and PVA integrated with CuO NPs synthesized via an ultrasonic-assisted green method using *S. ilicifolium* extract [18]. The physicochemical properties, morphological features, and thermal stability of the composite scaffolds are systematically evaluated to confirm nanoparticle incorporation and scaffold integrity [22]. Furthermore, the *in vitro* wound healing potential is assessed using a scratch assay on HaCaT keratinocyte cells to examine the scaffolds' ability to enhance cellular migration—a key event in tissue repair [23].

This research addresses the urgent need for innovative wound dressings that combine biocompatibility, bioactivity, and environmentally friendly synthesis methods. The use of *S. ilicifolium* not only provides a sustainable source for nanoparticle production but also adds intrinsic bioactivity to the system [24]. The starch/PVA nanofibrous scaffolds offer a conducive matrix for delivering CuO NPs effectively to the wound site, aiming to reduce infection risk while promoting faster wound closure [18]. The findings are expected to contribute valuable insights into the design of next-generation wound care materials that leverage marine bioresources and green nanotechnology.

2. MATERIALS AND METHODS

2.1. Collection and preparation of marine macroalgae

Brown macroalgae *S. ilicifolium* were manually gathered from the intertidal shores near Rameswaram, India. To preserve their bioactive constituents, the freshly collected specimens were placed in ice-cooled containers and promptly transported to the laboratory. On arrival, samples were rinsed under flowing tap water to eliminate surface sand, debris, and epiphytes, followed by repeated washes with distilled water for complete purification. Cleaned algal material was chopped into smaller fragments and air-dried under shaded conditions at ambient temperature for approximately two weeks. The dried biomass was finely ground using a mechanical mill to obtain a homogeneous powder, which was then stored in airtight containers at room temperature until extraction.

2.2. Ultrasonic-assisted extraction of bioactive compounds

To extract bioactive constituents, 2 grams of the powdered *S. ilicifolium* were mixed with 50 mL of Milli-Q water. The mixture underwent sonication using a LABQUEST ultrasonic cleaner (Borosil; Serial No. 941032329018) at 60°C for 45 minutes to enhance cell wall disruption and intracellular release. After sonication, the mixture was passed through sterile Whatman No. 1 filter paper to remove particulate matter, resulting in a clear extract. This filtrate was stored at 10°C for immediate use and subjected to lyophilization to obtain a dry extract powder for subsequent nanoparticle synthesis [25, 26].

2.3. Green synthesis of CuO NPs

CuO NPs were biosynthesized using the reducing agents in the algal extract of *S. ilicifolium*. Aqueous copper sulfate pentahydrate (0.1 M, 50 mL) was reacted with 10 mL of algal extract (prepared by dissolving 10 mg lyophilized extract in Milli-Q water). The 5:1 solution was magnetically stirred at 650 rpm and maintained at 60°C for 2 hours. A color transition from blue to bluish-green signified CuO NP formation. The reaction mixture was centrifuged, and the pellet was washed three times with double-distilled water to eliminate residual reactants and organic matter. The nanoparticles were then freeze-dried for 48 hours and preserved in a desiccator for later use in scaffold synthesis [27].

2.4. Fabrication of CuO-embedded starch/PVA nanofibrous mats via electrospinning

Electrospun mats were prepared by first dissolving PVA (15% w/w) in Milli-Q water under continuous stirring. Once fully dissolved, 100 mg of starch and 100 mg of biosynthesized CuO NPs were incorporated into the solution. The mixture was stirred at 50°C for 2.5 hours to ensure uniform dispersion. This homogenous blend was loaded into a syringe fitted with a stainless-steel needle (internal diameter: 0.84 mm) and mounted on a HOLMARC HO-NFES-040 electrospinning device. Parameters were optimized to 11.5 kV voltage, 12.3 cm distance, and 0.4 mL/h flow rate. Electrospinning continued at ambient temperature for 6–8 hours. The resulting nanofiber mats were gently peeled off and stored in a dry environment for subsequent analysis [28-30].

2.5. Physicochemical characterization of nanoparticles and nanofibrous scaffolds

2.5.1. UV-visible spectroscopy

Optical attributes and surface plasmon resonance (SPR) of both the CuO NPs and algal extract were assessed using a VIS SPEC V-730 UV-Vis spectrophotometer. Absorption spectra ranging from 200 to 800 nm were recorded using deionized water as blank. Peaks characteristic of CuO NP synthesis were evaluated and reported [31].

2.5.2. Fourier Transform Infrared Spectroscopy (FTIR)

FTIR spectroscopy was conducted in ATR mode with a PerkinElmer Spectrum Two instrument to detect functional groups in both nanoparticles and scaffold matrices. Spectra were collected between 4000–400 cm^{-1} with a resolution of 4 cm^{-1}, averaging 64 scans per sample. Key peaks corresponding to phenolic, hydroxyl, carbonyl, and metal-oxygen functional groups were interpreted [32].

2.5.3. X-Ray Diffraction (XRD)

The crystalline structure and purity of CuO NPs and scaffolds were examined via a Bruker D8 Advance XRD system using CuKα radiation (λ = 1.5406 Å), operating at 40 kV and 40 mA. Scans were carried out from 5° to 90° (2θ) with a 0.029649° step size. XRD peaks were compared with standard JCPDS reference data for phase confirmation [33].

2.5.4. Scanning Electron Microscopy (SEM)

Surface morphology and nanoparticle dispersion were visualized using a JEOL JSM-IT800 NANO SEM. Prior to imaging, specimens were sputter-coated with gold to enhance conductivity. Micrographs were analyzed for fiber arrangement, porosity, and nanoparticle distribution across the scaffolds [34].

2.5.5. Thermogravimetric Analysis (TGA)

Thermal degradation and compositional stability of the nanoscaffolds were investigated using a PerkinElmer TGA 8000 analyzer. Approximately 5 mg of each sample was heated from room temperature to 550°C at a 15°C/min ramp rate under nitrogen atmosphere. Thermal events such as moisture loss and polymer breakdown were recorded in thermograms [35].

2.5.6. Zeta potential and particle size

Zeta potential and hydrodynamic size distribution of CuO NPs were assessed using the Malvern Zetasizer Ultra. Stability of the colloidal nanoparticles was inferred from zeta potential values, with higher absolute values signifying enhanced electrostatic repulsion and dispersion stability [36].

All analytical data can be accessed on Mendeley Data using DOI: 10.17632/4kdtskdtmc.3.

2.6. Wound healing (scratch) assay

The *in vitro* scratch assay was used to determine the migration ability of HaCaT keratinocytes following exposure to test compounds: algal extract, CuO NPs, and starch/PVA/CuO-NP nanoscaffolds. Cells were plated in 12-well plates (2×10^5 cells/well) in DMEM supplemented with 10% FBS and 1% penicillin-streptomycin, and incubated at 37°C in 5% CO_2 to confluence. A sterile 200 µL tip was used to create a scratch simulating a wound. Wells were rinsed with PBS to remove debris and treated with various test samples at 6.25, 12.5, 25, 50, and 100 µg/mL in serum-free DMEM. Controls received no treatment. Cell migration and wound closure were monitored at 0, 24, and 48 hours using a phase-contrast inverted microscope. The percentage wound closure was quantified via ImageJ software to compare therapeutic efficiency across treatments [37].

2.7. Statistical analysis

All experiments were conducted in triplicate, and results were statistically evaluated using SPSS version 25.0 and GraphPad Prism version 9.0. Data are expressed as means ± standard deviations. One-way ANOVA was applied to identify significant intergroup differences, followed by post-hoc tests (Tukey's or Dunnett's). Statistical significance was accepted at $p < 0.05$. Pearson's correlation was used to examine relationships between parameters. Normality was assessed using the Shapiro–Wilk test, and non-normal datasets were log-transformed prior to further analysis. All conclusions were drawn at a 95% confidence level [38].

3. RESULTS

3.1. UV–visible spectroscopy

The optical properties (Fig. 1) of both the *S. ilicifolium* extract and the biosynthesized CuO NPs were analyzed using a JASCO V-730 UV-Visible spectrophotometer. The wavelength scan ranged from 200 to 800 nm with a 1 nm interval, employing continuous scanning mode and a 1.0 nm bandwidth. The seaweed extract exhibited distinct

absorption peaks characteristic of its phytochemical profile. In contrast, the CuO NPs demonstrated pronounced SPR bands, which confirmed the formation of metal oxide nanoparticles. Deionized water was used as the reference blank for baseline correction, ensuring accurate spectral data. The comparative analysis of these spectra confirms the successful biogenic synthesis of CuO NPs and highlights the extract's bioactive components.

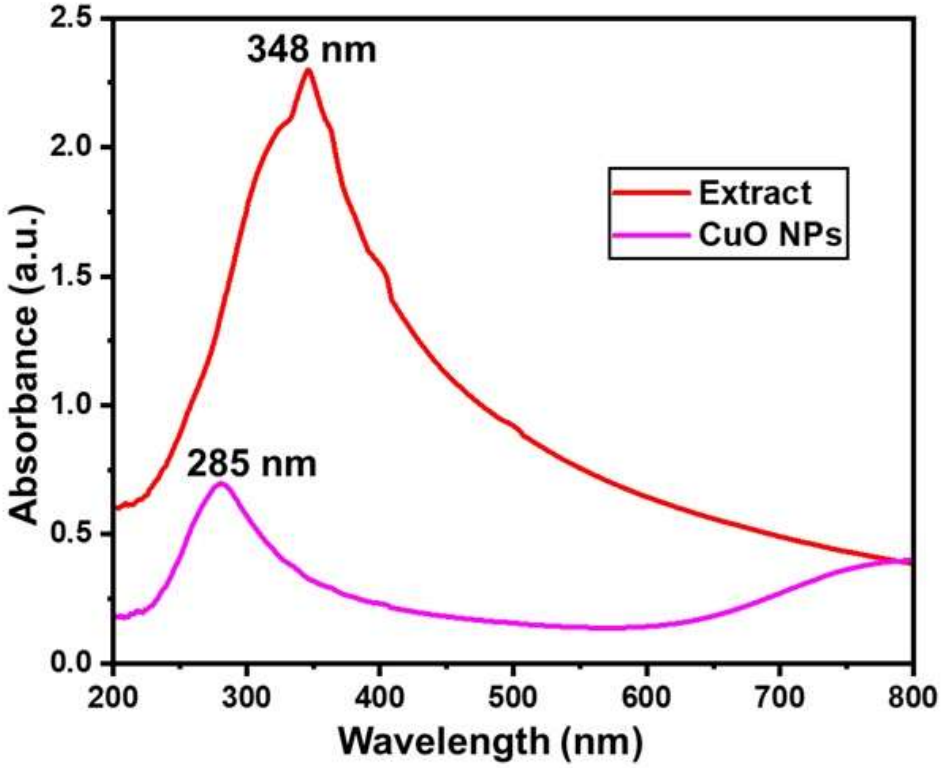

Fig. 1. UV–Visible spectral profiles of algal extract and CuO NPs.

3.2. FTIR analysis

FTIR spectroscopy (Fig. 2) was conducted to investigate the chemical functionalities of the CuO NPs and the starch/PVA electrospun scaffolds. Spectra were collected in ATR mode using a PerkinElmer Spectrum IR system over the range 4000–400 cm^{-1} with 4 cm^{-1} resolution, averaging 64 scans per sample. The CuO NPs presented characteristic absorption peaks at 3128.62, 2001.38, 1651.25, 1205.19, 866.65, and 599.74 cm^{-1}, indicative of Cu–O bonds and other surface groups. The starch/PVA scaffolds revealed distinct bands at 3297.43 cm^{-1} (O–H stretching), 1710.65 cm^{-1} (C=O carbonyl), 919.77 cm^{-1} (C–O–C polysaccharide linkage), and 842.91 cm^{-1} (C–H bending), confirming the polymeric and carbohydrate components. Observed shifts and broadening of peaks suggest effective interaction between the CuO NPs and the polymer matrix via hydrogen bonding and coordination with phenolic, hydroxyl, and carbonyl groups.

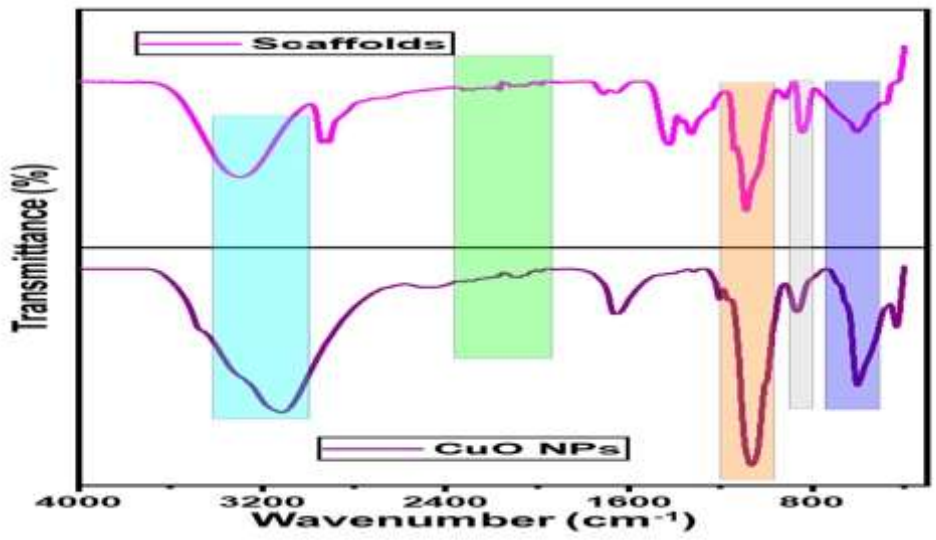

Fig. 2. FTIR spectra of CuO NPs and their incorporation into nanoscaffolds.

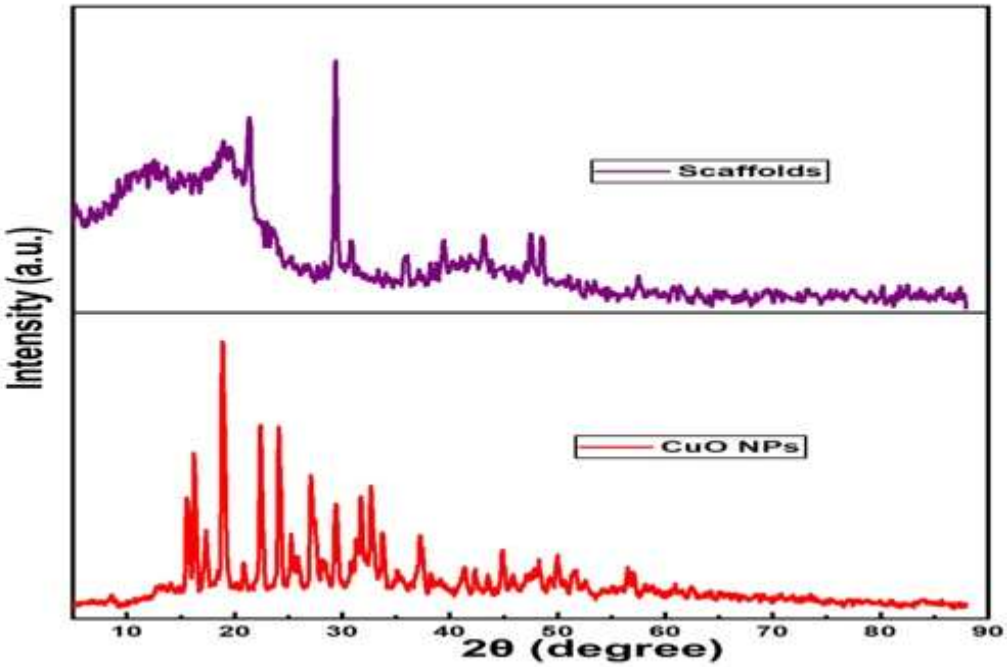

Fig. 3. XRD patterns of synthesized CuO NPs and CuO-loaded scaffolds.

3.3. XRD analysis

XRD patterns (Fig. 3) for the CuO NPs and starch/PVA nanofibrous scaffolds were recorded using a Bruker D8 Advance diffractometer with CuKα radiation (λ = 1.5406 Å) operated at 40 kV and 40 mA. The CuO NPs exhibited sharp diffraction peaks at 2θ values of 16.258°, 22.278°, 26.286°, 28.070°, 29.112°, 32.792°, 37.236°, 44.982°, 48.168°, 51.879°, and 53.557°, corresponding well with the monoclinic CuO crystalline phase according to JCPDS card 80-1917. The crystallite sizes were estimated via the Scherrer equation. The starch/PVA nanoscaffolds displayed broad diffraction peaks centered around 21.676°, 29.202°, 30.751°, 35.842°, 39.237°, 43.073°, 47.427°, 48.386°, and 57.535°, indicative of a semi-crystalline nature with d-spacing between 4.09671 Å and 1.60059 Å. Narrow peak widths in the CuO NPs (FWHM 0.198°–0.861°) suggest high crystallinity, while the broader peaks of the scaffold (FWHM 0.100°–0.658°) imply reduced crystallinity due to polymer presence. These results confirm the purity of the CuO phase and its successful integration into the starch/PVA matrix within a scanning range of 5° to 90°.

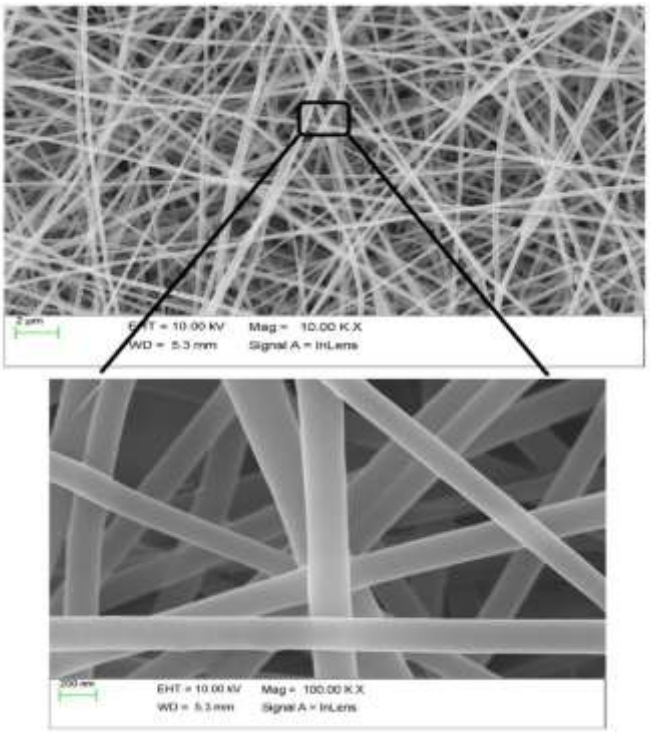

Fig. 4. SEM analysis of synthesized CuO NPs and CuO-loaded scaffolds.

3.4. SEM analysis

Surface morphology (Fig. 4) of the synthesized CuO NPs and electrospun starch/PVA scaffolds was examined through SEM using a JEOL JSM-IT800 NANO microscope. Prior to imaging, samples were sputter-coated with a thin layer of gold to enhance conductivity. SEM images of the CuO NPs revealed clusters composed of spherical to irregularly shaped particles with rough textures, characteristic of crystalline metal oxides. The starch/PVA nanoscaffolds exhibited a uniform, porous fibrous network with consistent fiber diameters and smooth surfaces. Minimal bead defects were observed, indicating effective polymer blending and optimized electrospinning conditions. These morphological insights support the potential application of these materials in biomedical fields such as wound healing and catalysis.

3.5. TGA

Thermal stability (Fig. 5) of the electrospun starch/PVA scaffolds was assessed by TGA using a PerkinElmer TGA 8000 instrument. Approximately 3.110 mg of sample was heated from 30°C to 550°C at a heating rate of 15°C/min under nitrogen flow. Initial weight loss started around 232.27°C, corresponding to moisture evaporation and early polymer degradation. The peak degradation rate was observed at 327.56°C, with major decomposition completing near 374.23°C. The total mass loss was calculated to be 38.301%. These thermal events indicate that the scaffolds possess significant thermal resistance and predictable degradation profiles suitable for biomedical use.

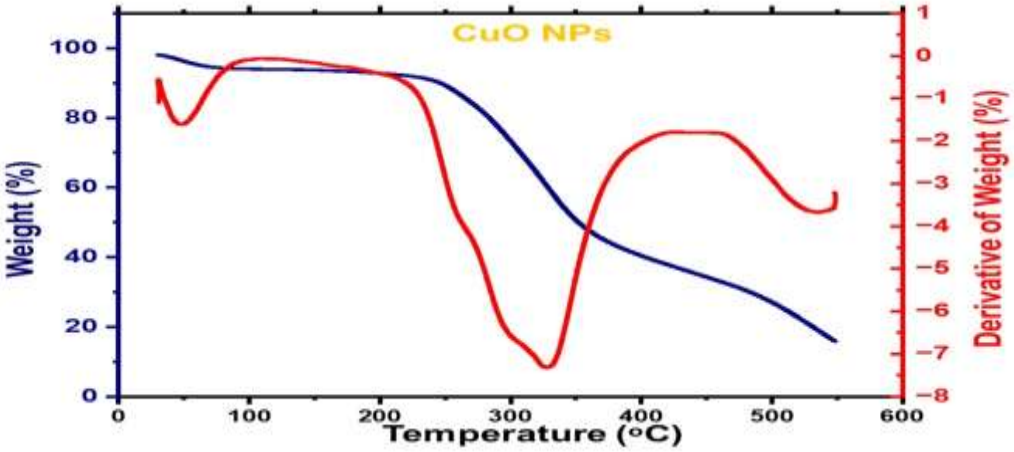

Fig. 5. Thermal degradation behavior of CuO-incorporated nanoscaffolds.

3.6. Zeta potential and particle size analysis

Dynamic light scattering (DLS) and zeta potential measurements were conducted on the CuO NPs using a Malvern Zetasizer Ultra at 25°C. The hydrodynamic diameter (Z-average) was determined to be 137 nm (Fig. 6), while the polydispersity index (PDI) was 0.7317, indicating a moderately broad size distribution. The zeta potential showed a mean value of −18.3 mV, with secondary peaks at −29.14 mV and −14.58 mV (Fig. 7), reflecting moderate electrostatic repulsion and colloidal stability. The measured suspension conductivity was 0.05074 mS/cm, and the quality factor of 5.22 validated the measurement's reliability. These findings demonstrate moderate nanoparticle dispersion stability and size heterogeneity, which are beneficial for their proposed biomedical and catalytic applications.

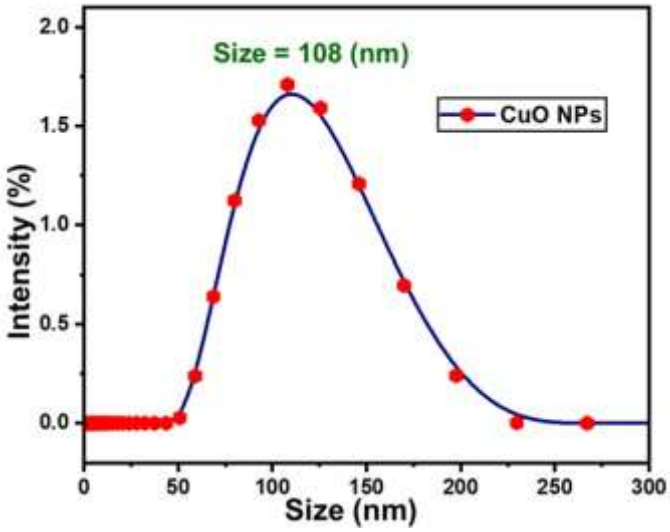

Fig.6. DLS particles size analysis of CuO NPs

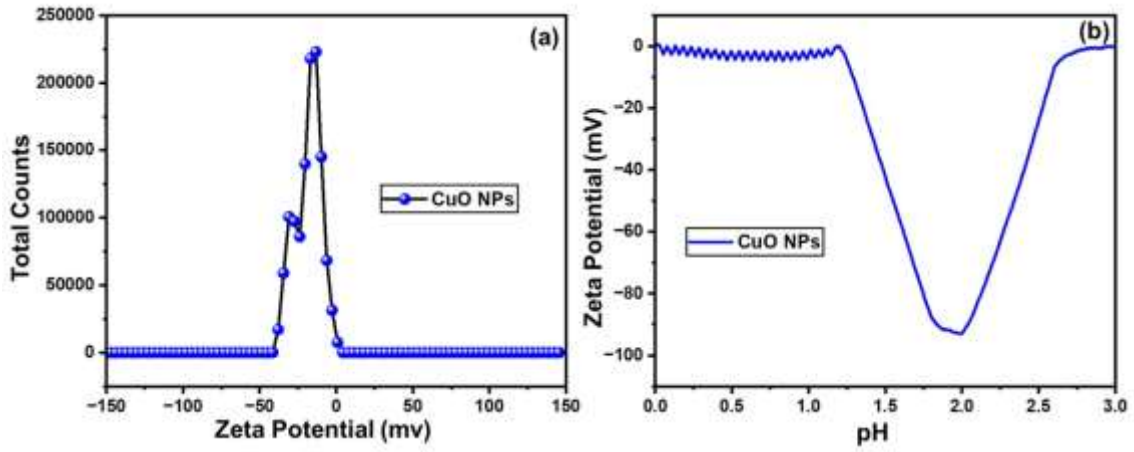

Fig.7. Zeta-potential analysis of CuO NPs

3.7. Wound healing (scratch) assay

After 48 hours of treatment, the wound healing assay (Fig. 8) demonstrated significant differences in cell migration among the test samples—algal extract, CuO NPs, and starch/PVA/CuO-NPs nanoscaffolds—across varying concentrations (6.25–100 µg/mL). At the lowest concentration (6.25 µg/mL), the algal extract exhibited a wound closure rate of 32.17%, while CuO NPs and nanoscaffolds showed higher closure rates of 40.17% and 47.17%, respectively. This trend persisted at 12.5 µg/mL, where the algal extract achieved 39.17% closure, compared to 46.17% for CuO NPs and 62.17% for nanoscaffolds, indicating a concentration-dependent enhancement in migratory activity.

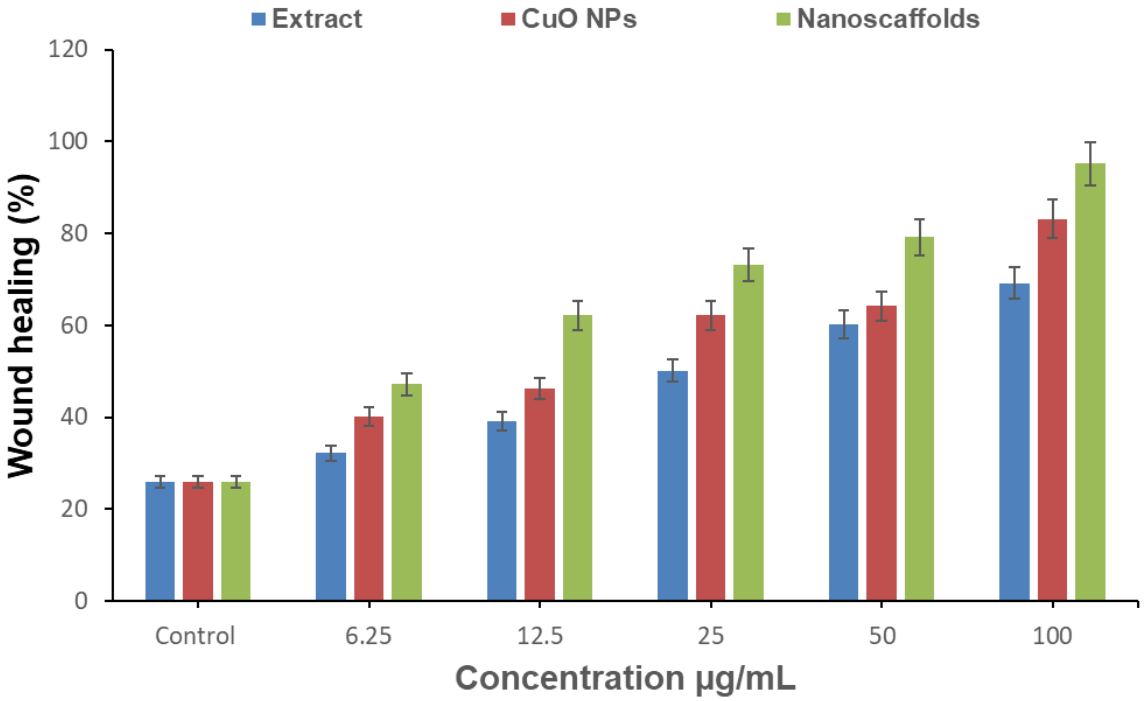

Fig. 8. Wound healing activity analysis of algal extract, CuO-NPs and starch/PVA/CuO-NPs nanoscaffolds

At intermediate concentrations (25–50 µg/mL), the nanoscaffolds consistently outperformed the other treatments. For instance, at 25 µg/mL, the nanoscaffolds induced 73.17% wound closure, surpassing the algal extract (50.17%) and CuO NPs (62.17%). Similarly, at 50 µg/mL, the nanoscaffolds reached 79.17% closure, while the algal extract and CuO NPs achieved 60.17% and 64.17%, respectively. The highest concentration (100 µg/mL) further highlighted the superior efficacy of nanoscaffolds, with 95.17% wound closure, compared to 69.17% for the algal extract and 83.17% for CuO NPs.

These results suggest that the starch/PVA/CuO-NPs nanoscaffolds significantly enhance HaCaT cell migration, likely due to their composite structure, which may provide a favorable microenvironment for cell proliferation

and movement. CuO NPs also exhibited notable activity, though less pronounced than the nanoscaffolds, while the algal extract showed moderate wound healing potential. The data underscore the potential of nanoscaffolds as a promising therapeutic agent for accelerating wound repair.

4. DISCUSSION

The UV–Visible spectroscopic analysis provided vital insights into the optical characteristics of both the *S. ilicifolium* extract and the biosynthesized CuO NPs. The distinctive absorption peaks observed in the seaweed extract correspond to its rich phytochemical composition, which includes various bioactive molecules such as polyphenols and flavonoids known for their reducing and stabilizing abilities. The CuO NPs demonstrated a pronounced SPR band, which is characteristic of metal oxide nanoparticles and confirms their successful synthesis. The use of deionized water as a blank and baseline correction ensured the precision of the measurements. These spectral data highlight not only the formation of CuO NPs but also the important role of biomolecules in the algal extract that facilitate the green synthesis route. This eco-friendly approach potentially avoids harmful chemicals and supports sustainable nanomaterial production [39-44].

FTIR analysis further elucidated the chemical interactions underlying the nanocomposite formation. The CuO NPs exhibited absorption peaks attributed to Cu–O bonds and associated surface functional groups, confirming the metal oxide framework. In parallel, the starch/PVA scaffolds revealed characteristic polymeric bands, including broad O–H stretches from hydroxyl groups, carbonyl C=O stretches, and polysaccharide linkages, indicating the presence of both starch and PVA components. The observed peak shifts and broadenings in the nanocomposite spectra imply strong interfacial interactions between the CuO NPs and the polymer matrix. Such interactions likely involve hydrogen bonding and coordination with hydroxyl, carbonyl, and phenolic groups originating from both the biomolecules of the extract and the polymers. This molecular level integration is crucial for enhancing the mechanical integrity and functional properties of the nanoscaffolds, ensuring uniform dispersion and stable embedding of CuO NPs within the fibrous network [45-51].

XRD patterns provided further confirmation of the structural attributes of the synthesized materials. The CuO NPs displayed sharp, well-defined peaks corresponding to the monoclinic crystalline phase, consistent with standard reference data. This high crystallinity is essential for many functional applications, including antimicrobial activity and catalytic efficiency, where ordered lattice structures often enhance performance. Conversely, the starch/PVA scaffolds exhibited broader diffraction peaks indicative of their semi-crystalline nature. The polymers' amorphous regions contribute to this broadening, reflecting the flexible and partially ordered arrangement of molecular chains. Importantly, the presence of CuO NPs did not disrupt the scaffold's structure but was successfully incorporated, as evidenced by the coexistence of characteristic peaks from both components. The semi-crystalline nature of the scaffolds ensures adequate mechanical flexibility, which is beneficial for wound dressing applications requiring conformability to wound contours [52-59].

Morphological examination using SEM revealed detailed surface characteristics essential for understanding the physical behavior of the materials. The CuO NPs formed aggregates with rough surfaces and variable shapes ranging from spherical to irregular, features typical of biogenically synthesized metal oxides. Such morphology can enhance surface area, contributing positively to antimicrobial and catalytic activities by providing more reactive sites. The starch/PVA nanoscaffolds, in contrast, exhibited a uniform, interconnected fibrous architecture with smooth, bead-free fibers. This morphology indicates optimized electrospinning parameters and effective polymer blending, critical factors for achieving high porosity and surface area conducive to cell attachment and nutrient diffusion in biomedical scaffolds. The porous fibrous network also facilitates moisture management, an essential aspect for efficient wound healing [60-64].

TGA shed light on the thermal stability and degradation behavior of the electrospun scaffolds. The initial weight loss around 232°C corresponds to moisture evaporation and early-stage polymer decomposition, while the major degradation peak at 327°C reflects the breakdown of polymer chains and organic constituents. The relatively high thermal stability and predictable decomposition pattern affirm that these scaffolds can maintain structural integrity under physiological and sterilization conditions, a prerequisite for biomedical applications. The total mass loss around 38% indicates the presence of stable polymeric and inorganic components, which is desirable to sustain scaffold functionality over the wound healing timeline [65-71].

DLS and zeta potential measurements provided crucial information on nanoparticle size distribution and colloidal stability. The hydrodynamic diameter of approximately 137 nm suggests that the nanoparticles are within the optimal nanoscale range for biomedical use, facilitating cellular uptake and interaction. The moderately broad polydispersity index indicates some size variability, which is common in green synthesis methods due to the complex nature of biological extracts. The zeta potential values, centered around −18.3 mV with secondary peaks, indicate moderate electrostatic repulsion among particles, contributing to colloidal stability. This stability is vital to prevent nanoparticle aggregation, which can adversely affect bioavailability and efficacy. The measured conductivity and quality factor further validate the robustness of these measurements. Overall, these nanoparticle characteristics reinforce their potential suitability in therapeutic and catalytic roles [72-76].

The wound healing assay demonstrated the significant biological efficacy of the developed nanoscaffolds in promoting HaCaT keratinocyte migration, a key process in wound closure. Across all tested concentrations, the starch/PVA/CuO-NPs nanoscaffolds consistently exhibited superior wound closure rates compared to both the algal extract and the CuO NPs alone. This enhanced activity is likely due to the synergistic effect of the polymeric

scaffold providing a conducive microenvironment combined with the bioactive CuO NPs that can modulate cellular behavior. The dose-dependent increase in closure percentage highlights the scaffolds' effectiveness at even low concentrations, which is advantageous for reducing potential cytotoxicity. The scaffold's porous structure may facilitate better cell attachment and proliferation, while the sustained release of CuO NPs may stimulate cellular responses necessary for tissue regeneration. The algal extract, rich in phytochemicals, showed moderate activity, reinforcing its role in nanoparticle synthesis and contributing bioactive compounds. These findings collectively suggest that the multifunctional starch/PVA/CuO nanoscaffolds hold promising therapeutic potential as advanced wound dressings capable of accelerating healing processes [77-80].

5. CONCLUSION

This study successfully demonstrated the green synthesis of CuO NPs using *S. ilicifolium* extract via an ultrasonic-assisted method, followed by their incorporation into starch/PVA electrospun nanoscaffolds for enhanced wound healing. Comprehensive characterization confirmed the formation of crystalline, monoclinic CuO NPs with favorable colloidal stability and thermal resistance. The nanoscaffolds exhibited a uniform, porous structure, facilitating cell adhesion and migration. *In vitro* scratch assays revealed that the starch/PVA/CuO-NPs nanoscaffolds significantly accelerated wound closure (95.17% at 100 µg/mL) compared to standalone CuO NPs (83.17%) and algal extract (69.17%), highlighting their superior bioactive potential. The synergistic interaction between biogenic CuO NPs and the polymeric matrix enhanced cell proliferation and migration, making these nanoscaffolds a promising wound dressing material. This study underscores the potential of eco-friendly, seaweed-mediated nanoparticle synthesis combined with electrospun nanofibers for advanced wound care applications, offering a sustainable and effective therapeutic approach for tissue regeneration.

Ethical Approval: Not Applicable for this study

Funding: No funding available for this study

Competing Interests: The authors declare that they have no conflict of interest.

Availability of data and materials: The full dataset of physiochemical characterization associated with this work is published in Mendeley Data **[Dataset]** Innovative green composites: Material characterization of starch-based nanoscaffolds reinforced with *Sargassum ilicifolium*-mediated copper oxide nanostructures (DOI: 10.17632/4kdtskdtmc.2). Disclosure: The material characterization data and figures (e.g., UV, SEM, FTIR, XRD, TGA, Zeta Potential and particle sizer) presented here were generated from a common dataset and are being reused across multiple related studies on nanomaterials. All biological analyses and conclusions are original to each manuscript.

REFERENCES

[1] Huang Y, Guo H, Liu Y, Jin W, Palanisamy CP, Pei J, Oz F, El-Aty AMA. Effects of Natural Polysaccharides on the Gut Microbiota Related to Human Metabolic Health. Molecular Nutrition & Food Research. 2025; 69:e202400792.

[2] Poornima K, Meenakshi K.C, Manikandan V.R, Shankari G, Prabhu D, Rathi M.A, Palanisamy CP, Balaji R, Gopalakrishnan V.K. Exploring the anticancer potential of Jerantinine A from *Tabernaemontana coronaria* against prostate, breast, and ovarian cancers: A computational approach. *Journal of Complementary and Integrative Medicine*, 2025 22(2): 363–372.

[3] Palanisamy CP, Poompradub S, Sansanaphongpricha K, Jayaraman S, Subramani K. Faridah Sonsudin gGreen synthesis of Nigella sativa-mediated silver nanoparticles for enhanced antibacterial activity and wound healing: Mechanistic insights and biomedical applications. Environmental Nanotechnology, Monitoring & Management. 2025; 24: 101085.

[4] Surendran N, Raju MV, Chandrasekaran MK, Ahalliya RM, Palanisamy CP, Chandrasekaran G, Kanniappan GV. Physicochemical characterization of starch from Maranta arundinacea L.(arrowroot) rhizomes and its inhibition of COX-2: In vivo validation. Bioactive Carbohydrates and Dietary Fibre. 2025; 33: 100465.

[5] Kannappan P, Chandrasekaran MK, Raju MV, Gopalakrishnan S, Dhamodharan P, Ahalliya RM, Palanisamy CP, Raju B, Kanniappan GV. Exploring the anticancer potential of Jerantinine A from Tabernaemontana coronaria against prostate, breast, and ovarian cancers: a computational approach. Journal of Complementary and Integrative Medicine. 2025; 22(02): 363-372.

[6] Pei J, Kumarasamy RV, Jayaraman S, Kanniappan GV, Long Q, Palanisamy CP. Quercetin-functionalized nanomaterials: Innovative therapeutic avenues for Alzheimer's disease management. Ageing Research Reviews. 2025; 104: 102665.

[7] Jayaraman S, Prasad M, Natarajan SR, Krishnamoorthy R, Alshuniaber MA, Gatasheh MK, Veeraraghavan VP, Rajagopal P, Palanisamy CP. Molecular mechanisms underlying the effects of beta-sitosterol on TGF-β1/Nrf2/SIRT1/p53-mediated signaling in the kidney of a high-fat diet and sucrose-induced type-2 diabetic rat. Chemico-Biological Interactions. 2025; 411: 111443.

[8] Huang Y, Guo H, Liu Y, Jin W, Palanisamy CP, Pei J, Oz F, El-Aty AMA. Effects of Natural Polysaccharides on the Gut Microbiota Related to Human Metabolic Health. Molecular Nutrition & Food Research. 2025; e202400792.
[9] Prabhakaran P, Palanisamy CP, Shanmugam A, Damodharan P, Swaminathan H, Devaraj D, Ahalliya RM, Kanniappan GV. Isolation, structural characterization, and molecular docking studies on the bioactive compound from n-Hexane extract of Emilia sonchifolia (L.) DC against the pancreatic cancer target Aurora 2 Kinase. Journal of Complementary and Integrative Medicine. 2024; 22(1): 0290.
[10] Jiang H, Kumarasamy RV, Pei J, Raju K, Kanniappan GV, Palanisamy CP. Integrating engineered nanomaterials with extracellular vesicles: Advancing targeted drug delivery and biomedical applications. Frontiers in Nanotechnology. 2024; 6: 1513683.
[11] Guo H, Liu Y, Wan T, Song D, Palanisamy CP, Geng J, Pei J, Özmen S, El-Aty AMA. Toward personalized cancer management: Role of precision nutrition–diet interventions. Journal of Functional Foods. 2024; 123: 106584.
[12] Natarajan SR, Krishnamoorthy R, Alshuniaber MA, Al-Anazi KM, Farah MA, Rajagopal P, Palanisamy CP, Veeraraghavan VP, Jayaraman S. Identification of FOXM1 as a novel protein biomarker and therapeutic target for colorectal cancer progression: Evidence from immune infiltration and bioinformatic analyses. International Journal of Biological Macromolecules. 282 (Part 4): 137201.
[13] Rajendran MS, Jayaraman S, Khan JM, Jasmine S, Prabhakaran RK, Raju MV, Chandrasekaran MK, Ahalliya RM, Kannappan P, Palanisamy CP, Kanniappan GV. Investigating the colon toxicity and carcinogenic role of monosodium glutamate compared with Dimethylhydrazine in male Wistar rats: Exploring the link to childhood colon cancer risk. Journal of King Saud University - Science. 2024; 36(11): 103507.
[14] Kumarasamy RV, Natarajan P, Umapathy VR, Roy JR, Rab SO, Saeed M, Panagal M, Mironescu M, Srinivasan GP, Palanisamy CP. Clinical Applications and Therapeutic Potentials of Advanced Nanoparticles: A Comprehensive Review on Completed Human Clinical Trials. Frontiers in Nanotechnology. 2024; 6:1479993.
[15] Jin W, Pei JJ, Roy JR, Jayaraman S, Ahalliya RM, Kanniappan GV, Mironescu M, Palanisamy CP. Comprehensive review on single-cell RNA sequencing: A new frontier in Alzheimer's disease research. Ageing Research Reviews. 2024; 274: 102454.
[16] Pei J, Palanisamy CP, Jayaraman S, Natarajan PM, Umapathy VR, Roy JR, Panagal M, Jayaraman S. Curcumin-loaded polymeric nanomaterials as a novel therapeutic strategy for Alzheimer's disease: A comprehensive review. Ageing Research Reviews. 2024; 99: 102393.
[17] Pei J, Palanisamy CP, Jayaraman S, Natarajan PM, Umapathy VR, Roy JR, Thalamati D, Ahalliya RM, Kanniappan GV, Mironescu M. A comprehensive review on starch-based Sustainable Edible Films Loaded with Bioactive Components for Food Packaging. International Journal of Biological macromolecules. 2024; 274 (Part-1): 133332.
[18] Palanisamy CP, poompradub S, Sansanaphongpricha K, Subramani K, Sonsudin F. Increased expression levels of PDGF and VEGF magnify the wound healing potential facilitated by biogenic synthesis of silver nanoparticles. Nano-Structures & Nano-Objects. 2024; 39: 101236.
[19] Pei J, Palanisamy CP, Jayaraman S, Natarajan PM, Umapathy VR, Roy JR, Thalamati D, Ahalliya RM, Kanniappan GV, Mironescu M. Proteomics Profiling of Extracellular Vesicle for Identification of Potential Biomarkers in Alzheimer's Disease: A Comprehensive Review. Ageing Research Reviews. 2024; 99: 102359.
[20] Xi J, Wang T, Xian P, Liu X, Du M, Yang H, Palanisamy CP, Lin W, Long Q. Proteomic insights uncover enhanced neurotherapeutic potential in conditioned mesenchymal stem cell-derived extracellular vesicles. Extracellular Vesicle. 2024; 3: 100037.
[21] Pei J, Natarajan PM, Umapathy VR, Swamikannu B, Sivaraman NM, Krishnasamy L, Palanisamy CP. Advancements in the synthesis and functionalization of zinc oxide-based nanomaterials for enhanced oral cancer therapy. Molecules. 2024; 29(11): 2706.
[22] Gatasheh MK, Natarajan SR, Krishnamoorthy R, Alsulami TS, Rajagopal P, Palanisamy CP, Veeraraghavan VP, Jayaraman S. Molecular analysis to identify novel potential biomarkers as drug targets in colorectal cancer therapy: an integrated bioinformatics analysis. Molecular and Cellular Oncology. 2024; 11(1): 2326699.
[23] Pei J, Yan Y, Jayaraman S, Rajagopal P, Natarajan PM, Umapathy VR, Gopathy S, Roy JR, Sadagopan CS, Thalamati D, Palanisamy CP, Mironescu M. A review on advancements in the application of starch-based nanomaterials in biomedicine: Precision drug delivery and cancer therapy. International Journal of Biological Macromolecules. 2024; 130746.
[24] Pei JJ, Yan Y, Palanisamy CP, Jayaraman S, Natarajan PM, Umapathy VR, Gopathy S, Roy JR, Sadagopan JC, Thalamati D, Mironescu M. Materials-based drug delivery approaches: Recent advances and future perspectives. Green Processing and Synthesis. 2024; 13: 20230094.
[25] Pei JJ, Deng W, Liu Y, Guo Y, Chen J, Abdu H, Khan MR, Palanisamy CP, El-Aty AM. A Comprehensive Review of Cornus officinalis: Health Benefits, Phytochemistry, and Pharmacological Effects for Functional Drug and Food Development. Frontiers in Nutrition. 2023; 10: 1309963.
[26] Natarajan PM, Umapathy VR, Murali A, Swamikannu B. (2022). Computational Simulations of Identified marine-derived Natural Bioactive Compounds As Potential Inhibitors of Oral Cancer. Future Science OA. 2022; 8(3).

[27] Natarajan PM, Umapathy VR. Role of transcriptomics in the study of oral cancer. Frontiers in Oral Health. 2025; 6:1524364.
[28] Vidhyarekha U, Natarajan PM, Bhuminathan S, Sabarinathan J, Suba R, Vijayalakshmi P. Role of artificial intelligence in Oral Cancer. Advances in Public Health. 2024. 2024: 3664408.
[29] Ganesan A, Kumar NG, Natarajan PM, Gauthaman J. Automated classification of elongated styloid processes using deep learning models-an artificial intelligence diagnostics. Frontiers in Oral Health. 2025; 5: 1424840.
[30] Umapathy VR, Natarajan PM, Swamikannu B. Regenerative Strategies in Dentistry: Harnessing Stem Cells, Biomaterials and Bioactive Materials for Tissue Repair. Biomolecules. 2025; 15: 546.
[31] Natarajan PM. Dental Bioinformnatics-Current Scope and Future perspectives. Research Journal of Pharmacy and Technology. 2022;15(5):2351-6.
[32] Ganesan A, Kumar NG, Natarajan PM. Solanum trilobatum leaf extract-derived silver nanoparticles downregulate the PI3K/AKT/mTOR signaling pathway and attenuate oral squamous cell carcinoma cell proliferation. Journal of Herbmed Pharmacology. 2024; 13(2): 300-307.
[33] Perumal MKK, Renuka RR, Subbiah SK, Natarajan PM. Artificial intelligence-driven clinical decision support systems for early detection and precision therapy in oral cancer: a mini review. Frontiers in Oral Health. 2025; 6: 1592428.
[34] Ramesh E, Ganesan A, Lakshmi KC, Natarajan PM. Artificial intelligence-based diagnosis of oral leukoplakia using deep convolutional neural networks Xception and MobileNet-v2. Frontiers in Oral Health. 2025; 6: 1414524.
[35] Ganesan A, Kumar NG, Natarajan PM. Anticancer activity of silver nanoparticles synthesized from aqueous leaf extract of Solanum trilobatum (Purple fruit pea eggplant) on human oral cancer cells. Journal of Herbmed Pharmacololgy. 2024; 13(2): 260-268.
[36] Pei JJ, Perumal NC, Meng P, Long Q, Palanisamy CP. AI-assisted FTIR spectroscopic profiling of exosomes: Emerging frontiers in early detection of Alzheimer's disease. Ageing Research Reviews. 2026; 103311.
[37] Raja FSD, Abraham L, Rangasamy K, Saikia K, Rathankumar AK, Mironescu M, Mironescu I, Palanisamy CP, Kanniappan GV. Next-Generation Microbiome Therapeutics: Psychobiotics and Fecal Microbiota Transplants (FMT) for Mental Health Treatment. Frontiers in Cellular and Infection Microbiology. 2026; 16: 1719357.
[38] Subramani K, Srinivasan S, Shanmugam P, Palanisamy CP, Sonsudin F, Poompradub S. Sustainable phytochemical mediated-ZnO nanoparticles derived from Crescentia cujete for toxicological evaluation and multifunctional environmental applications. Environmental Nanotechnology, Monitoring & Management. 2026; 26: 101180.
[39] Kunamalla RP, Panagal M, Palanisamy CP. Green-engineered multiscale starch/PVA nanofibrous scaffolds embedded with CuO nanoparticles from Sargassum ilicifolium for potent antimicrobial performance. Genetics and Molecular Research. 2026; 25(13s): 1-9.
[40] Dharmaprakash S, Gunasekaran VP, Sivaramakrishnan R, Kanniappan GV, Jayaraman S, Mironescu M, Rajabathar JR, Mironescu ID, Palanisamy CP. Marine macroalgae-mediated ultrasonic-assisted green synthesis of CuO nanoparticles embedded in starch/PVA electrospun nanoscaffolds for in vitro α-amylase and α-glucosidase inhibitory activity. Scientific Reports. 2026; 16: 26243.
[41] Surendran N, Chandrasekaran G, Raju MV, Chandrasekaran MK, Ahalliya RM, Palanisamy CP, Kanniappan GV, Arcot R, Alharbi NS, Thiruvengadam M. Anti-inflammatory potential of ethanolic extract of Maranta arundinacea L.: Insights from COX-2 modulation and oxidative stress analysis. South African Journal of Botany. 2026; 195: 142-151.
[42] Pei J, Senthilkumar MV, Hessini K, Subramaniyam S, Sivaramakrishnan R, Kanniappan GV, Jayaraman S, Palanisamy CP. Green fabrication of starch/PVA/CuO nanoscaffolds using marine macroalgae extract for enhanced anti-inflammatory activity. Sustainable Chemistry and Pharmacy. 2026; 51: 102397.
[43] Balasubramanian V, Loganathan L, Muthuswamy K, Viswanathan TM, Raju MV, Chandrasekaran MK, Ahalliya RM, Poorasamy J, Palanisamy CP, Dominic S, Kanniappan GV. Anticancer therapeutic efficacy of PEGylated β-galactosidase from Aspergillus terreus in DMBA-induced breast cancer: Toxicological, molecular and histopathological evaluation in Wistar rats. International Journal of Biological Macromolecules. 2026; 360: 151856.
[44] Jayaraman S, Eswaran A, Rajagopal P, Palanisamy CP, Veerakumar P, Veeraraghavan VP, Sirasanagandla SR. Neuroendocrine-associated epigenetic factors in cellular senescence: mechanisms and therapeutic implications. Biogerontology. 2026; 27(2): 64.
[45] Ponnusamy B, Rajagopal P, Palanisamy CP, Veeraraghavan VP, Jayaraman S. Mechanistic Exploration of the anticancer activity of Justicia adhatoda Plant Leaf Ethanolic Extract against Colon Cancer Cells: An in silico and in vitro Approach. Asian Pacific Journal of Cancer Prevention. 2026; 27(3): 1069-1080.
[46] Pei J, Saran VS, Sivaramakrishnan R, Kanniappan GV, Pandurangan V, Jayaraman S, Dhayalan VK, Mironescu M, Mironescu ID, Palanisamy CP. Ultrasonic-assisted, Sargassum ilicifolium (brown marine macroalgae)-mediated biogenic synthesis of CuO nanoparticles incorporated in starch/PVA electrospun nanoscaffolds: In vitro safety and antioxidant efficacy assessment. Bioorganic Chemistry. 2026; 173: 109679.

[47] Raj MAPA, Subramaniyam S, Kanniappan GV, Jayaraman S, Palanisamy CP. Sustainable fabrication of starch/PVA/CuO electrospun nanoscaffolds from Turbinaria ornata (marine macroalgae) extract: Physicochemical characterization and antidiabetic evaluation. Kuwait Journal of Science. 2026; 53(2): 100545.
[48] Pei J, Ganesh NS, Subramaniyam S, Sivaramakrishnan R, Kanniappan GV, Jayaraman S, Palanisamy CP. Sustainable fabrication of starch/PVA/CuO electrospun nanoscaffolds from Padina tetrastromatica (Brown macroalgae) extract: Physicochemical characterization and antidiabetic assessment. Sustainable Chemistry One World. 2026; 9: 100195.
[49] Sakthiraj A, Sivaramakrishnan R, Subramaniyam S, Kanniappan GV, Pandurangan V, Jayaraman S, Dhayalan VK, Mironescu M, Mironescu ID, Palanisamy CP. Starch/PVA electrospun nanoscaffolds loaded with ultrasonic-assisted green-synthesis of CuO nanoparticles from marine macroalgae (Gracilaria corticata) extract: Cytotoxicity and antioxidant analysis. Chemical Physics Impact. 2026; 12: 101018.
[50] Raju M, Chandrasekaran MK, Loganathan L, Ahalliya RM, Mironescu M, Mironescu ID, Palanisamy CP, Kanniappan GV. Lipid remodeling and ferroptosis in phosphatidylcholine-mediated tumor–stroma crosstalk. Frontiers in Molecular Biosciences. 2026; 13: 1742305.
[51] Kunamalla R, Panagal M, Palanisamy CP. Biogenic synthesis and fabrication of starch/PVA/CuO electrospun nanoscaffolds from Sargassum ilicifolium (brown marine macroalgae) extract for anticancer activity on HT-29 and MCF-7 cancer cells. Biocatalysis and Agricultural Biotechnology. 2026; 72: 103923.
[52] Pei J, Govindaraj H, Sivaramakrishnan R, Kanniappan GV, Pandurangan V, Dhayalan VK, Mironescu M, Mironescu ID, Jayaraman S, Palanisamy PC. Sustainable fabrication of biopolymer-based (starch/PVA) nanoscaffolds loaded with green-synthesized CuO nanoparticles from Sargassum wightii (marine macroalgae): Cytocompatibility and antioxidant activity. Biomaterials Advances. 2026; 182: 214660.
[53] Pei J, Perumal NC, Meng P, Long Q, Palanisamy CP. Extracellular vesicle-based biosensors for Alzheimer's disease: A new frontier in precision diagnostics. Ageing Research Reviews. 2026; 113: 102904.
[54] Shree P, Sivaramakrishnan R, Kanniappan GV, Pandurangan V, Jayaraman S, Dhayalan VK, Mironescu M, Mironescu ID, Palanisamy CP. Antioxidant and biocompatible CuO-starch/PVA nanoscaffolds via ultrasonic green synthesis using Turbinaria conoides (brown marine macroalgae). Medicine in Drug Discovery. 2025; 28: 100238.
[55] Gong J, Lin J, Guan T, Pei J, Palanisamy CP, El-AtyFrom AMA. selenium tolerance to nanoplastic antagonism: Comprehensive characterization of L. casei SNUT1 and its extracellular vesicle–nanoselenium complex. Food Bioscience. 2025; 74: 107749.
[56] Poochi SP, Sundarraj R, Raju MV, Chandrasekaran MK, Ahalliya RM, Palanisamy CP, Kanniappan GV, Kondapavuluri BK, Thiruvengadam M. Harnessing Nature: Computational and Experimental Insights Into *Ipomoea obscura* Metabolites for Bladder Cancer Therapy. Chemistry and Biodiversity. 2025; 0: e00909.
[57] Dugganaboyana GK, Kannankumar MKG, Shivaramakrishna S, Raju MV, Chandrasekaran MK, Ahalliya RM, Panneerselvam N, Palanisamy CP, Kanniappan GV. Phytochemical insights, antioxidant activity and therapeutic potential of Cassia senna against prostate cancer in Wistar albino rats. Discover Applied Sciences. 2025; 7:1206.
[58] Natarajan SR, Krishnamoorthy R, Alshuniaber MA, Gatasheh MK, Rajagopal P, Veeraraghavan VP, Palanisamy CP, Jayaraman S. KDM1A Facilitates Oncogenic Potential in Colorectal Cancer Progression Through the Activation of AXIN/GSK3β/β-Catenin Signaling Pathways: Evidence From Integrated Transcriptomics and In Vitro Studies. The Journal of Gene Medicine. 2025; 27(11): e70053.
[59] Guan T, Gong J, Lin J, Palanisamy CP, Jinjin Pei J, El-Aty AMA. Machine learning-driven multimodal optimization of selenium biotransformation and flavor profiling in fermented apple–Yacon functional beverages. Innovative Food Science & Emerging Technologies. 2025; 105: 104198.
[60] Natarajan SR, Krishnamoorthy R, Alshuniaber MA, Alsulami TS, Gatasheh MK, Rajagopal P, Palanisamy CP, Govindan R, Veeraraghavan VP, Jayaraman S. ABCE1 facilitates tumour progression via aerobic glycolysis and inhibits cell death in human colorectal cancer cells through the p53 signalling pathway. Scientific Reports. 2025; 15: 24674.
[61] Natarajan PM, Swamikannu B, Sivaraman NM, Stylin AGSQ. Prevention of Oral Cancer: A Comprehensive Guide. Journal of Pharmacy and Bioallied Sciences. 2024; 16(5): S4239-S4241.
[62] Umapathy V, Dhanavel A, Kesavan R, Natarajan PM, Bhuminathan S, Vijayalakshmi P. Anticancer Potential of the Principal Constituent of Piper nigrum, Piperine: A Comprehensive Review. Cureus. 2024; 16(2): e54425.
[63] Umapathy VR, Swamikannu B, Natarajan PM, Devi R, Nandini MS, Vimalarani, Vijayalakshmi P. In Silico Molecular Docking of Ocimum sanctum Phytochemicals: Targeting Key Biomarkers in Oral Cancer. Journal of Pharmacy and Bioallied Sciences. 2024; 16(5): S4792-S4799.
[64] Natarajan PM, Bhuminathan S, Rajan R, Bindu K, Loganathan K, Veerakumar R. The Crucial Role of Smoking Cessation in Preventing Oral Cancer. Journal of Pharmacy and Bioallied Sciences. 2024; 16(5): S4245-S4247.
[65] Swamikannu B, Umapathy VR, Natarajan PM, Nandini MS, Stylin AGSQ, Vimalarani V, Rajinikanth S. Unlocking the Therapeutic Benefits of Artemisia Annua: A Comprehensive Overview of its Medicinal Properties. Journal of Pharmacy and Bioallied Sciences. 2024; 16(5): S4248-S4253.
[66] Natarajan PM. Computational Studies on Recent Congeners of Fluoroquinolones and Nitroimidazoles for Their Use in Periodontal Therapy. Journal of Pharmacy and Bioallied Sciences. 2024; 16(5): S4731-S4740.

[67] Yadalam PK, Arumuganainar D, Natarajan PM, Ardila CM. Artificial intelligence-powered prediction of AIM-2 inflammasome sequences using transformers and graph attention networks in periodontal inflammation. Scientific Reports. 2025; 15: 8733.
[68] Yadalam PK, Chatterjee S, Natarajan PM, Ardila CM. Comparison of light gradient boosting and logistic r egression for interactomic hub genes in Porphyromonas gingivalis and Fusobacterium nucleatum-induced perio dontitis with Alzheimer's disease. Frontiers in Oral Health. 2025; 6:1463458.
[69] Natarajan PM, Bhuminathan S, Leela B, Bindu K, Loganathan K, Ramachandran V. Smoking and its Role in Oral Cancer. Journal of Pharmacy and Bioallied Sciences 16(5): S4242-S4244.
[70] Yadalam PK, Natarajan PM, Ardila CM. Variational graph autoencoder for reconstructed transcriptomic data associated with NLRP3 mediated pyroptosis in periodontitis. Scientific Reports. 2025; 15: 1962.
[71] Alugoju P, Palanisamy CP, Anthikapalli NVA, Jayaraman S, Prasanskulab A, Chuchawankul S, Dyavaiah M, Tencomnao T. Exploring the anti-aging potential of natural products and plant extracts in budding yeast Saccharomyces cerevisiae: A review. F1000Research. 2023; 12: 1265.
[72] Lavanya M, Krishnamoorthy R, Alshuniaber MA, Manoharadas S, Palanisamy CP, Veeraraghavan VP, Jayaraman S, Rajagopal P, Padmini R. Formulation, characterization and evaluation of gelatin-syringic acid/zinc oxide nanocomposite for its effective anticancer, antioxidant and anti-inflammatory activities. Journal of King Saud University-Science. 2023; 35: 102909.
[73] Palanisamy CP, Poompradub S, Sansanaphongpricha K, Jayaraman S, Subramani K, Sonsudin F. Biosynthesis of silver nanoparticles (AgNPs) using ethanolic extract of Nigella sativa (L.) seeds promotes wound healing via PDGF and VEGF signalling pathways activation. Biocatalysis and Agricultural Biotechnology. 2023; 54: 102970.
[74] Prasad M, Jayaraman S, Natarajan SR, Veeraraghavan VP, Krishnamoorthy R, Gatasheh MK, Palanisamy CP, Elrobh M. Piperine modulates IR/Akt/GLUT4 pathways to mitigate insulin resistance: Evidence from animal and computational studies. International Journal of Biological Macromolecules. 2023; 253: 127242.
[75] Palanisamy CP, Pei JJ, Phaniendra A, Venkata AAN, Jayaraman S, Veeraragahavan VP, Sridevi G, Roy JR, Janaki CS, Thalamati D, Mironescu M, Luo Q, Chai Y, Long Q. New Strategy of Neurodegenerative Disease Treatment with Extracellular Vesicles (EVs) Derived from Mesenchymal Stem Cells (MSCs). *Theranostics*. 2023; 13(12):4138-4165. doi:10.7150/thno.83066.
[76] Palanisamy CP, Phaniendra A, Jayaraman S, Poompradub S. *Nigella sativa* L. seed extracts promotes wound healing progress by activating VEGF and PDGF signalling pathways: *An in vitro* and *in silico* study. *F1000 Research*. 2023; 12: 436.
[77] Pei JJ, Palanisamy CP, Phaniendra A, Venkata AAN, Natarajan PM, Umapathy VR, Swamikannu B, Jayaraman S, Rajagopal P, Poompradub S. A comprehensive review on bio-based materials for chronic diabetic wounds. *Molecules*. 2022; 28(2), 604.
[78] Palanisamy CP, Cui B, Zhang H, Gunasekaran VP, Ariyo A, Jayaraman S, Veeraraghavan V, Rajagopal P. A critical review on starch-based electrospun nanofibrous scaffolds for wound healing application. International Journal of Biological Macromolecules. 2022; 222 (Part: B): 1852-1860.
[79] Monisha P, Ponnulakshmi R, Nalini D, Vishnu P V, Palanisamy CP, Cui B, Shankargouda P, Selvaraj J. A comprehensive review on high fat diet-induced diabetes mellitus: An epigenetic view. The Journal of Nutritional Biochemistry. 2022; 2022: 109037.
[80] Monisha P, Selvaraj J, Mohamed AE, Mohamed E, Mosaab AEA, Vishnu PV, Srinivasan V, Vidhya RU, Shazia FJH, Kalaiselvi K, Durairaj S, Palanisamy CP, Surapaneni K M, Ponnulakshmi R. A Comprehensive review on therapeutic perspectives of phytosterols in insulin resistance: A mechanistic approach. Molecules. 2022; 27(5): 1595.